

## **SI MATERIALS AND METHODS**

### **Cell culture**

All cells were grown in RPMI 1640 containing 10% FBS and supplemented with 1X pen/strep and were passaged every 2-3 days (37°C and 5% CO<sub>2</sub>). For *in vivo* experiments, the MDA-MB-231 and H1703 cells were cultured up to the time of tail-vein or subcutaneous injections, respectively, when they were resuspended in plain RPMI 1640 medium only. All cell lines were confirmed mycoplasma negative using MycoFluor™ Mycoplasma Detection Kit (Thermo Fisher Scientific).

### **Quantitative real-time polymerase chain reaction (qPCR) analysis**

mRNAs were assayed using the TaqMan Gene Expression Assays in accordance with the manufacturer's instructions (Thermo Fisher Scientific). TaqMan probes for PHIP and HPRT1 were purchased from Thermo Fisher Scientific. The expression level of the human *PHIP* gene was normalized to the human *HPRT1* gene before comparisons.

### **Transfection of pcDNA3, TLN1 and PHIP plasmids**

To overexpress TLN1 or PHIP, a lipofectamine 2000-mediated transfection (9μL) of plasmid 26724 encoding *TLN1* cDNA (3μg) (Addgene), control pcDNA3 plasmid (3μg) (Thermo Fisher Scientific) or *PHIP* cDNA plasmid (ViGene Biosciences) was carried out by following the manufacturer's instructions (Thermo Fisher Scientific).

### **Western analysis**

The following antibodies were used: anti-human PHIP antibody (1:500 dil.; Abnova), anti-human ALK antibody (at 1:2000 dil.: Cell Signaling), anti-human AKT antibody (1:2000 dil.; Cell Signaling); anti-human phospho AKT antibody (at 1:500 dil.; Cell Signaling), anti-human lamin B1 (at 1:500 dil., Abcam), anti-human H4K91ac (at

1:500 dil., Abcam), anti-human GAPDH antibody (at 1:2000 dil.; EMD Millipore), anti-beta-Actin (at 1:5000 dil.; Sigma), goat anti-mouse HRP (at 1:2000 dil.; Bio-Rad) and bovine anti-rabbit HRP (at 1:2000 dil.; Bio-Rad). Protein extracts from H3122 and H2228 cells (Cell Signaling) were used as controls for ALK rearrangements.

### **Nuclear fractionation and co-immunoprecipitation**

The cells were harvested and lysed with a fractionation buffer (0.5% Triton X-100, 137.5mM NaCl, 10% glycerol, 1mM EDTA, 50mM Tris-HCl and protease and phosphatase inhibitor cocktail) for 20min on ice. Then, the cell lysate was centrifuged and the supernatant containing the cytoplasmic fraction was collected. Pelleted insoluble nuclei were lysed by using sonication in fractionation buffer containing protease and phosphatase inhibitor cocktail. For the co-immunoprecipitation, 1mg of nuclear protein extract was incubated overnight with anti-human PHIP (at 1 $\mu$ g; Bethyl Laboratories), anti-human H4K91ac (at 1 $\mu$ g; Abcam) or anti-rabbit IgG control (at 1 $\mu$ g; Santa Cruz Biotechnology) antibodies following the Current Protocols in Molecular Biology (Co-precipitating proteins with protein A/G sepharose).

### **Immunofluorescence and confocal imaging**

The following antibodies were used: anti-human PHIP (at 1:250 dil.; Abnova) and anti-PCNA (at 1: 500 dil., Leica Biosystems) were detected using a secondary antibody labeled with Alexa Fluor 594 (at 1:1000 dil.; Thermo Fisher Scientific). Antibodies against human H4K91ac (at 1:500 dil., Abcam), TLN1 (at 1:500 dil.; Abcam), CCND1 (at 1:1000 dil.; Santa Cruz Biotechnology), pHH3 (at 1:500 dil., EMD Millipore) and Ki67 (at 1:500 dil., Abcam) were detected using a secondary antibody labeled with Alexa Fluor 488 (at 1:1000 dil.; Thermo Fisher Scientific). Images were taken at fixed

exposures with a Zeiss Axio Image Z2 microscope and the fluorescence intensities of individual cells were quantified using ImageJ software. The mean pixel intensities were used for statistical analysis using Microsoft Excel and Data Desk. Confocal imaging was performed using a Zeiss LSM 880 with Airyscan detector. The system was controlled using Zeiss Zen 2 software and images were analyzed using Imaris software (Bitplane AG).

### **TCGA gene expression analyses**

The TCGA breast cancer RNA-Seq dataset consisted of 528 human samples. These samples were further subdivided into five subtypes based on their molecular profile (Normal-like, HER2-enriched, Luminal A, Luminal B and Basal-like) (1). Pairwise comparisons of *PHIP* gene expression within each of the subtypes for each cancer were performed using Welch's t-test analysis in R (2). Further Student's *t*-test analysis was performed to find differences in *PHIP* gene expression between triple-negative samples (ER negative, PR negative and HER2 negative) and other samples. The TCGA melanoma RNA-Seq dataset consisted of 332 human samples. The samples were further subdivided into four subtypes based on their molecular profile (*BRAF* hotspot mutations, any *NF1* mutations, *RAS* hotspot mutations, and triple wild-type (No *BRAF*, *NRAS*, *NF1*) (3). The TCGA lung cancer adenocarcinoma RNA-Seq dataset consisted of 230 human samples that were divided into three molecular subtypes (bronchioid, magnoid and squamoid) (4). Pairwise comparisons were performed to identify the enrichment of *PHIP* gene expression in any of the subtypes. Additionally, the samples with mutations in *KRAS*, *EGFR* and *ALK* were excluded from the dataset and pairwise comparison analyses were repeated.

## **Animal studies**

Groups of twelve 45-day-old female nude mice (Harlan) were injected i.v. with 500,000 MDA-MB-231 cells expressing anti-*luc* shRNA or anti-*PHIP* shRNA and the number of metastatic lung tumors was counted at sacrifice at day 36 post-injection. For the lung xenograft experiment, groups of ten 45-day-old female nude mice (Harlan) were injected with 5 million H1703 cells expressing anti-*luc* shRNA or anti-*PHIP* shRNA and tumor volume was measured at sacrifice at day 50 post-implantation. Based on published literature, groups of 10 to 12 mice were used to provide statistically significant data while keeping the number of animals to a minimum.

## **REFERENCES**

1. Cancer Genome Atlas N (2012) Comprehensive molecular portraits of human breast tumours. *Nature* 490(7418):61-70.
2. Welch BL (1947) The Generalization of 'student's' problem when several different population variances are involved. *Biometrika* 34(1-2):28-35.
3. Cancer Genome Atlas N (2015) Genomic Classification of Cutaneous Melanoma. *Cell* 161(7):1681-1696.
4. Cancer Genome Atlas Research N (2014) Comprehensive molecular profiling of lung adenocarcinoma. *Nature* 511(7511):543-550.

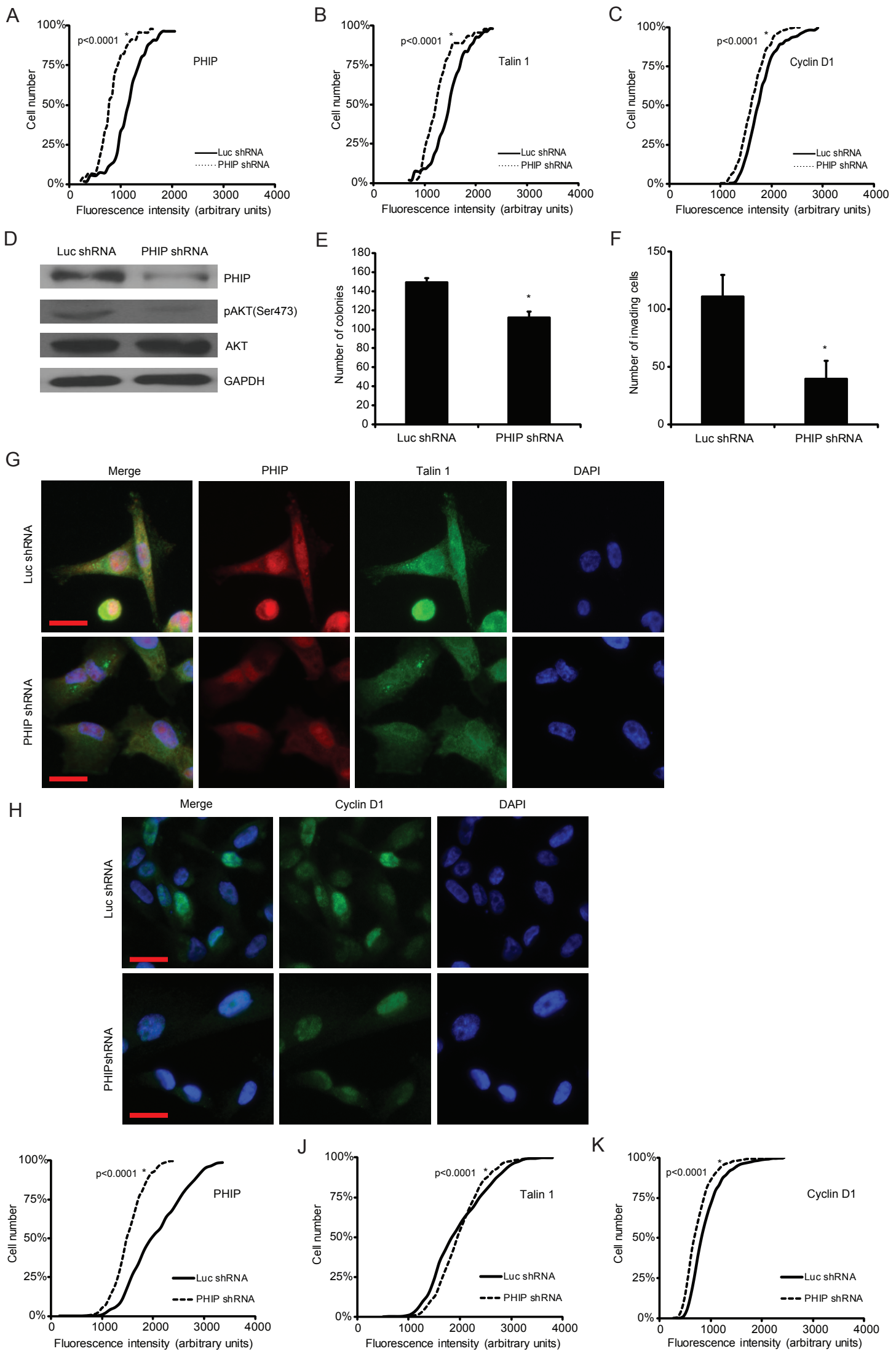


**Fig. S1.** Effects of stable shRNA-mediated suppression of *PHIP* in MDA-MB-231 cells. Quantitative immunofluorescence analysis of (A) PHIP, (B), Talin 1, and (C) Cyclin D1 expression in MDA-MB-231 cells expressing anti-*PHIP* shRNA or anti-*luc* shRNA (127738). (D) Western analysis of expression of PHIP and other proteins in MDA-MB-231 cells expressing anti-*luc* shRNA or a second anti-*PHIP* shRNA (130419). (E) Colony formation ability of MDA-MB-231 cells expressing anti-*luc* shRNA or anti-*PHIP* shRNA (130419) ( $P < 0.02$ ). (F) Invasion into Matrigel of MDA-MB-231 cells expressing anti-*luc* shRNA or anti-*PHIP* shRNA (130419) ( $P < 0.02$ ). (G-H) Qualitative immunofluorescence analysis of (G) PHIP and Talin 1 and (H) Cyclin D1 in MDA-MB-231 cells expressing anti-*luc* shRNA or anti-*PHIP* shRNA (130419) (scale bar, 20 $\mu$ m). (I-K) Quantitative immunofluorescence analysis of (I) PHIP, (J) Talin 1 and (K) Cyclin D1 in MDA-MB-231 cells expressing anti-*luc* shRNA or anti-*PHIP* shRNA (130419).

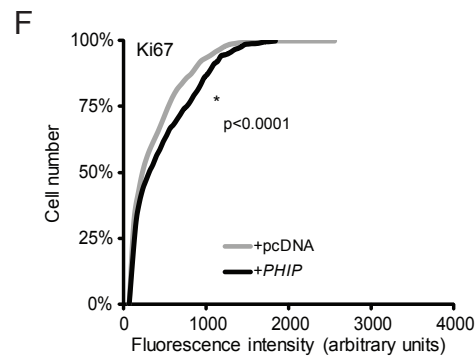
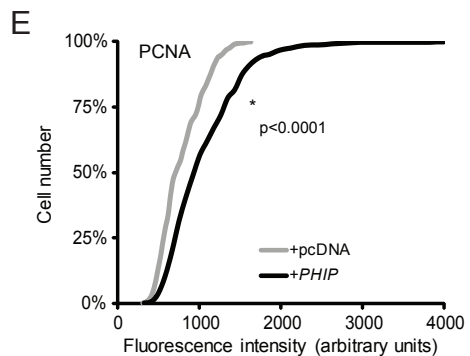
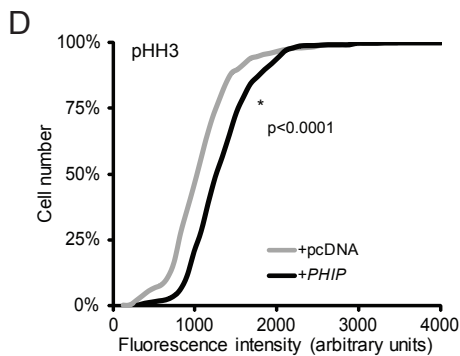
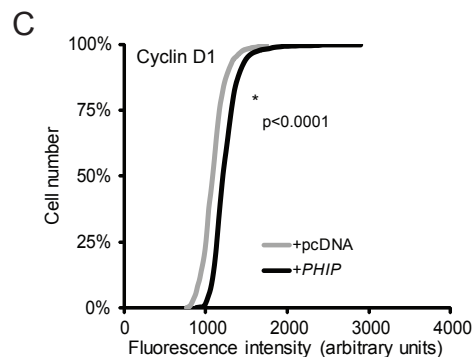
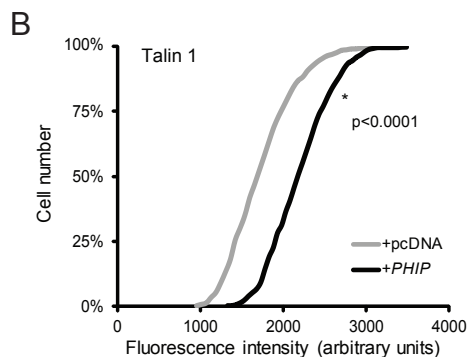
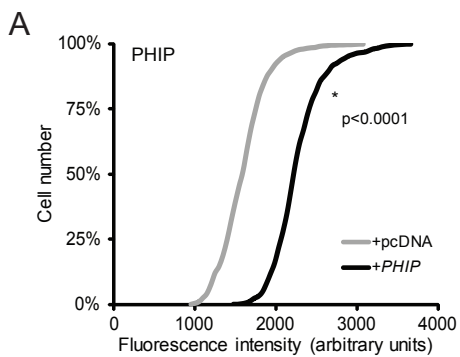


**Fig. S2.** Effects of modulation of *PHIP* expression in MDA-MB-231 cells. (A-F) Quantitative immunofluorescence analysis of (A) PHIP, (B) Talin 1, (C) Cyclin D1, (D) pHH3, (E) PCNA and (F) Ki67 in MDA-MB-231 cells overexpressing *PHIP* cDNA or control plasmid.



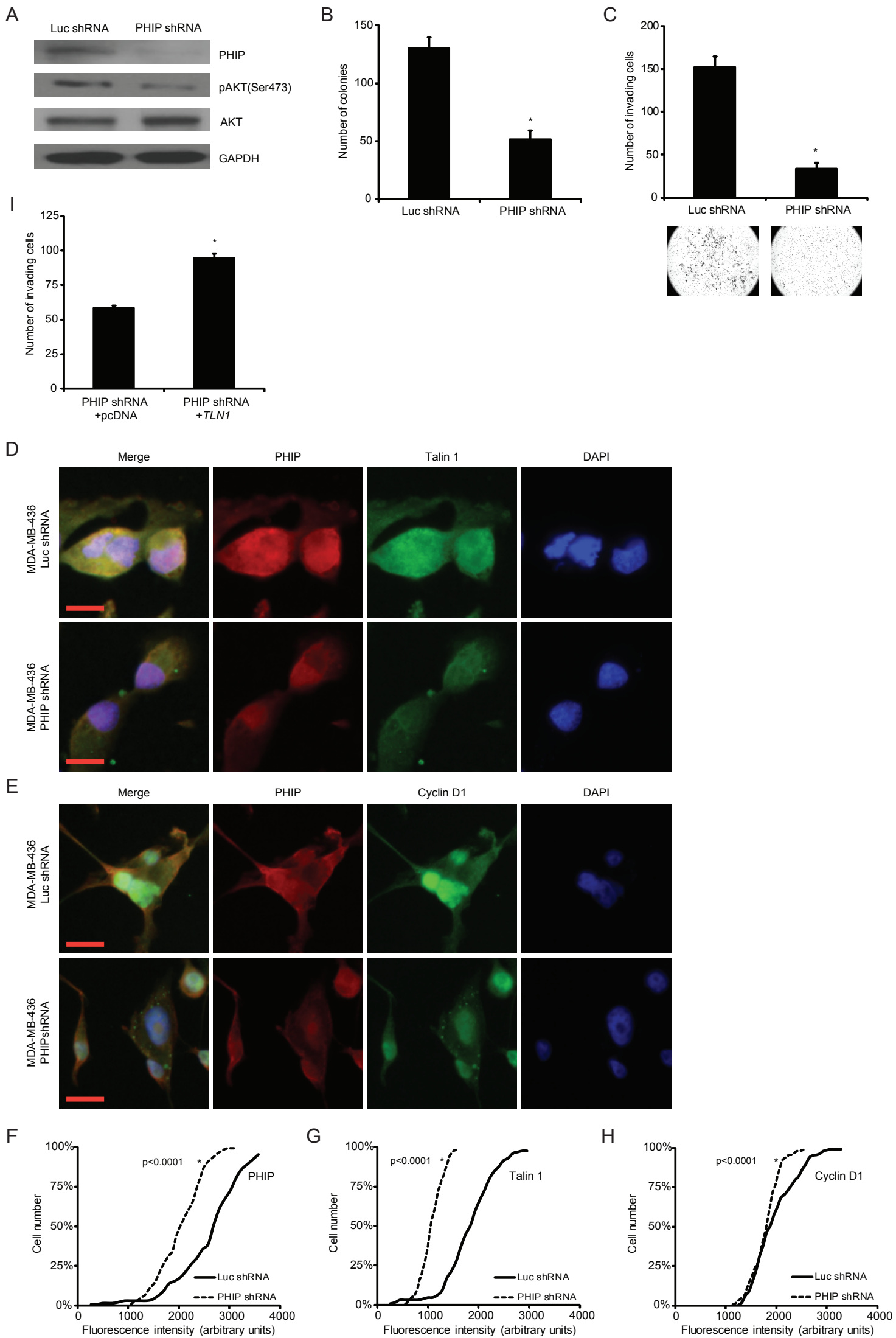


**Fig. S3.** Effects of stable shRNA-mediated suppression of *PHIP* in MDA-MB-436 cells. (A) Western analysis of expression of PHIP and other proteins in MDA-MB-436 cells expressing anti-*luc* shRNA or anti-*PHIP* shRNA (127738). (B) Colony formation ability of MDA-MB-436 cells expressing anti-*luc* shRNA or anti-*PHIP* shRNA (127738) ( $P < 0.0005$ ). (C) Invasion into Matrigel of MDA-MB-436 cells expressing anti-*luc* shRNA or anti-*PHIP* shRNA (127738) with corresponding microphotographs ( $P = 0.001$ ). (D-E) Qualitative immunofluorescence analysis of (D) PHIP and Talin 1 and (E) PHIP and Cyclin D1 in MDA-MB-436 cells expressing anti-*luc* shRNA or anti-*PHIP* shRNA (127738) (scale bar, 20 $\mu$ m). (F-H) Quantitative immunofluorescence analysis of (F) PHIP, (G) Talin 1 and (H) Cyclin D1 in MDA-MB-436 cells expressing anti-*luc* shRNA or anti-*PHIP* shRNA (127738). (I) Effects of overexpression of *TLN1* cDNA or control plasmid on invasive capacity into Matrigel of MDA-MB-436 cells expressing anti-*PHIP* shRNA (127738) ( $P = 0.01$ ).

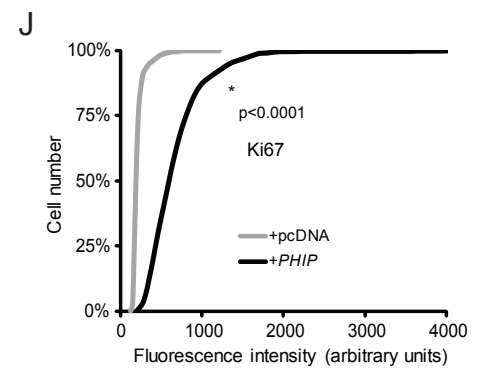
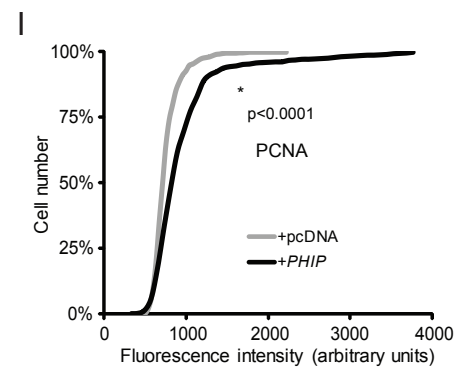
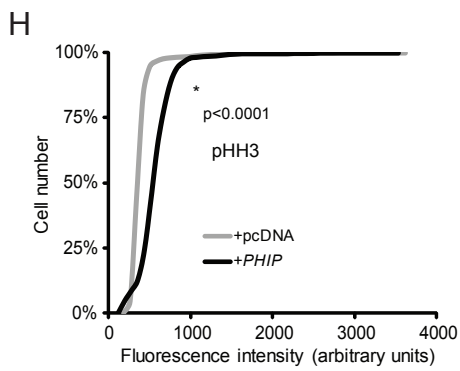
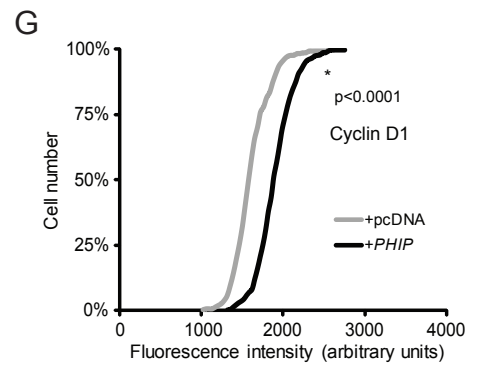
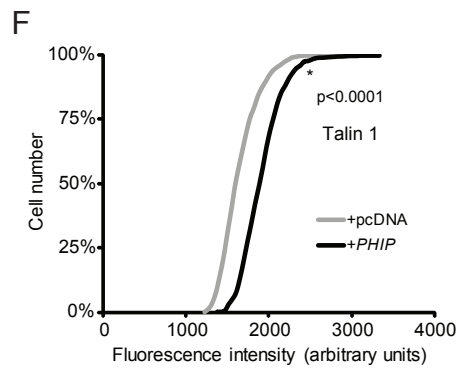
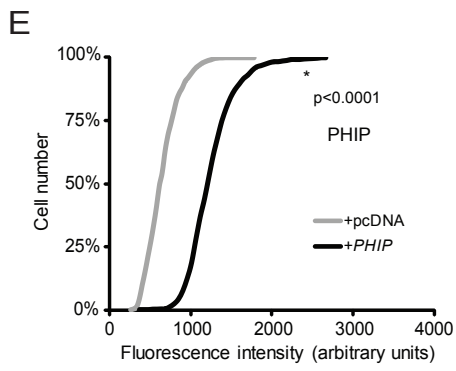
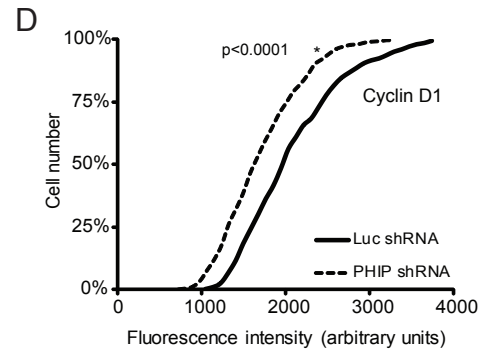
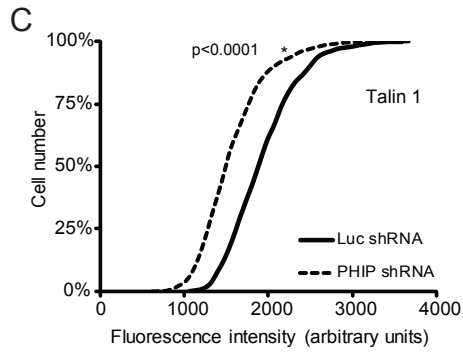
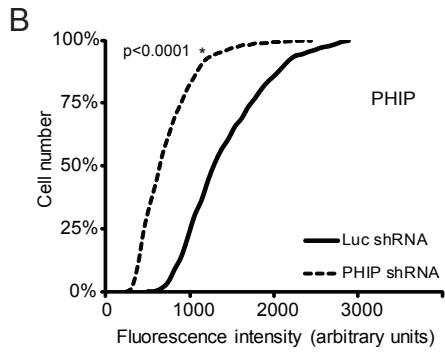
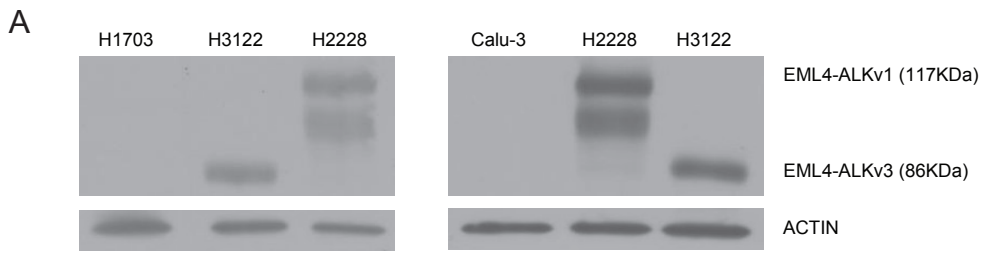


**Fig. S4.** ALK expression in lung cancer cells and effects of modulation of *PHIP* expression in H1703 cells. (A) Western analysis of ALK rearrangements and beta-actin in H1703 and Calu-3 cells compared to reference cells with specific EML4-ALK rearrangements (H2228 and H3122). (B-D) Quantitative immunofluorescence analysis of (B) PHIP, (C) Talin 1 and (D) Cyclin D1 in H1703 cells expressing anti-*Luc* shRNA or anti-*PHIP* shRNA (127738). (E-J) Quantitative immunofluorescence analysis of (E) PHIP, (F) Talin 1, (G) Cyclin D1, (H) pHH3, (I) PCNA and (J) Ki67 in H1703 cells overexpressing *PHIP* cDNA or control plasmid.

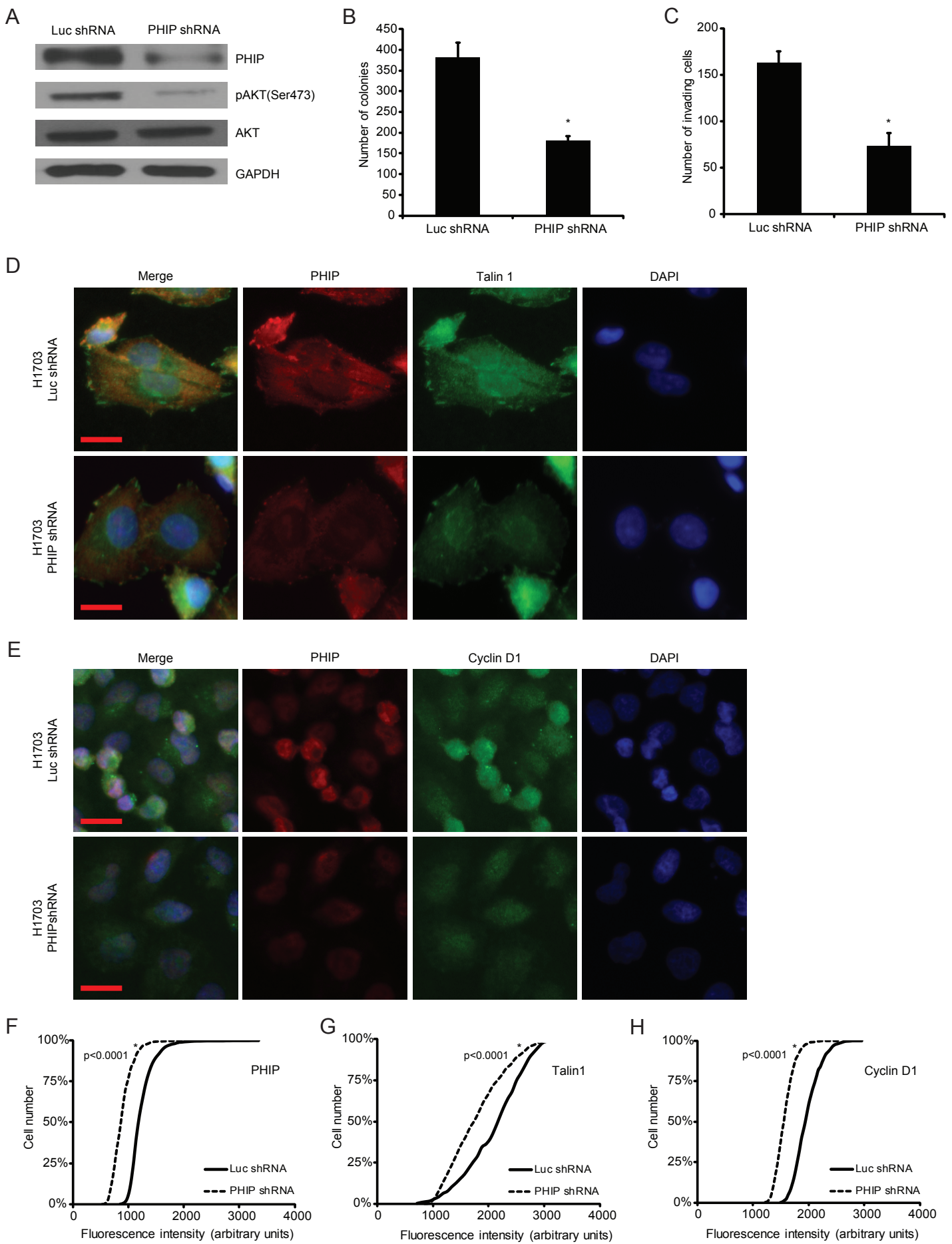


**Fig. S5.** Effects of stable shRNA-mediated suppression of *PHIP* in H1703 cells. (A) Western analysis of expression of PHIP and other proteins in H1703 cells expressing anti-*luc* shRNA or a second anti-*PHIP* shRNA (130419). (B) Colony formation ability of H1703 cells expressing anti-*luc* shRNA or anti-*PHIP* shRNA (130419) ( $P=0.005$ ). (C) Invasion into Matrigel of H1703 cells expressing anti-*luc* shRNA or anti-*PHIP* shRNA (130419) ( $P=0.0007$ ). (D-E) Qualitative immunofluorescence analysis of (D) PHIP and Talin 1 and (E) PHIP and Cyclin D1 in H1703 cells expressing anti-*luc* shRNA or anti-*PHIP* shRNA (130419) (scale bar, 20 $\mu$ m). (F-H) Quantitative immunofluorescence analysis of (F) PHIP, (G) Talin 1 and (H) Cyclin D1 in H1703 cells expressing anti-*luc* shRNA or anti-*PHIP* shRNA (130419).

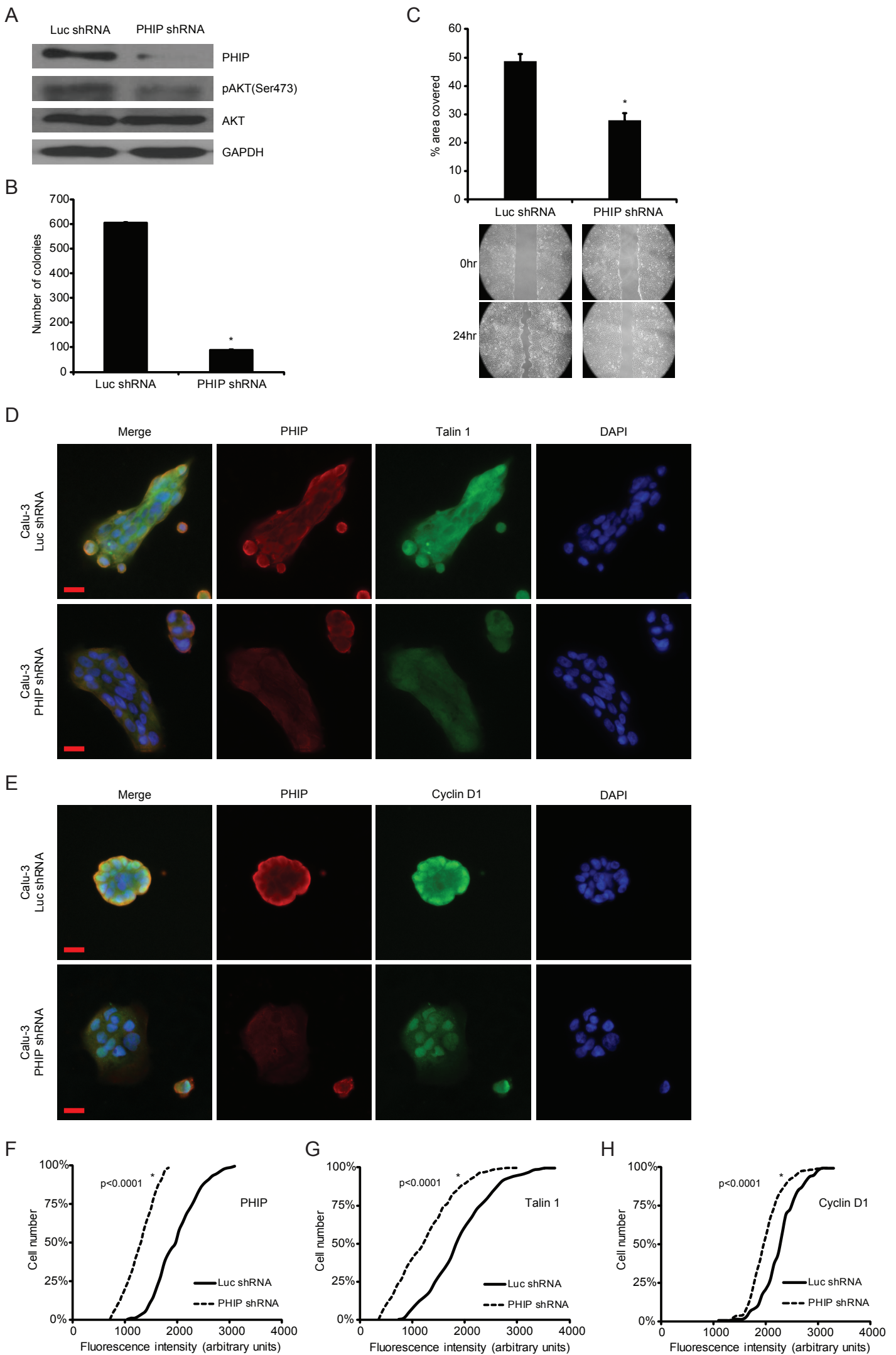


**Fig. S6.** Effects of stable shRNA-mediated suppression of *PHIP* in Calu-3 cells. (A) Western analysis of expression of PHIP and other proteins in Calu-3 cells expressing anti-*luc* shRNA or anti-*PHIP* shRNA (127738). (B) Colony formation ability of Calu-3 cells stably expressing anti-*luc* shRNA or anti-*PHIP* shRNA (127738) ( $P < 0.00000005$ ). (C) Wound closure at 24h post-scratch of Calu-3 cells expressing anti-*luc* shRNA or anti-*PHIP* shRNA (127738) with corresponding microphotographs (average of 5 scratches per cell line;  $P < 0.00005$ ). (D-E) Qualitative immunofluorescence analysis of (D) PHIP and Talin 1 and (E) PHIP and Cyclin D1 in Calu-3 cells expressing anti-*luc* shRNA or anti-*PHIP* shRNA (127738) (scale bar, 20 $\mu$ m). (F-H) Quantitative immunofluorescence analysis of (F) PHIP, (G) Talin 1 and (H) Cyclin D1 in Calu-3 cells expressing anti-*luc* shRNA or anti-*PHIP* shRNA (127738).



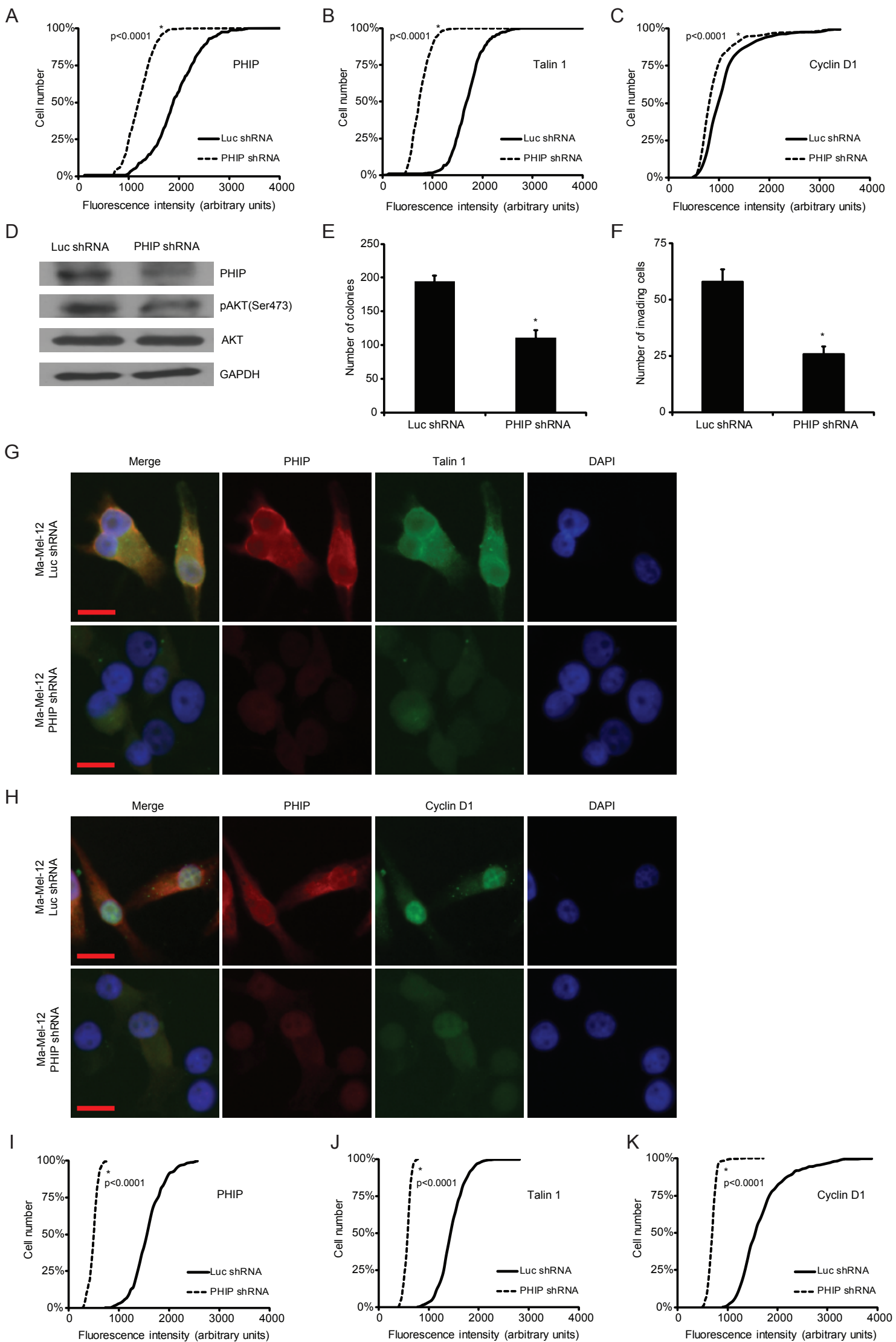


**Fig. S7.** Effects of shRNA-mediated suppression of *PHIP* in Ma-Mel-12 cells. (A-C) Quantitative immunofluorescence analysis of (A) PHIP, (B) Talin 1 and (C) Cyclin D1 in Ma-Mel-12 cells expressing anti-*luc* shRNA or anti-*PHIP* shRNA (127738). (D) Western analysis of expression of PHIP and other proteins in Ma-Mel-12 cells expressing anti-*luc* shRNA or a second anti-*PHIP* shRNA (130419). (E) Colony formation ability of Ma-Mel-12 cells stably expressing anti-*luc* shRNA or anti-*PHIP* shRNA (130419) ( $P=0.002$ ). (F) Invasion into Matrigel of Ma-Mel-12 cells expressing anti-*luc* shRNA or anti-*PHIP* shRNA (130419) ( $P=0.001$ ). (G-H) Qualitative immunofluorescence analysis of (G) PHIP and Talin 1 and (H) PHIP and Cyclin D1 in Ma-Mel-12 cells expressing anti-*luc* shRNA or anti-*PHIP* shRNA (130419) (scale bar, 20 $\mu$ m). (I-K) Quantitative immunofluorescence analysis of (I) PHIP, (J) Talin 1 and (K) Cyclin D1 in Ma-Mel-12 cells expressing anti-*luc* shRNA or anti-*PHIP* shRNA (130419).

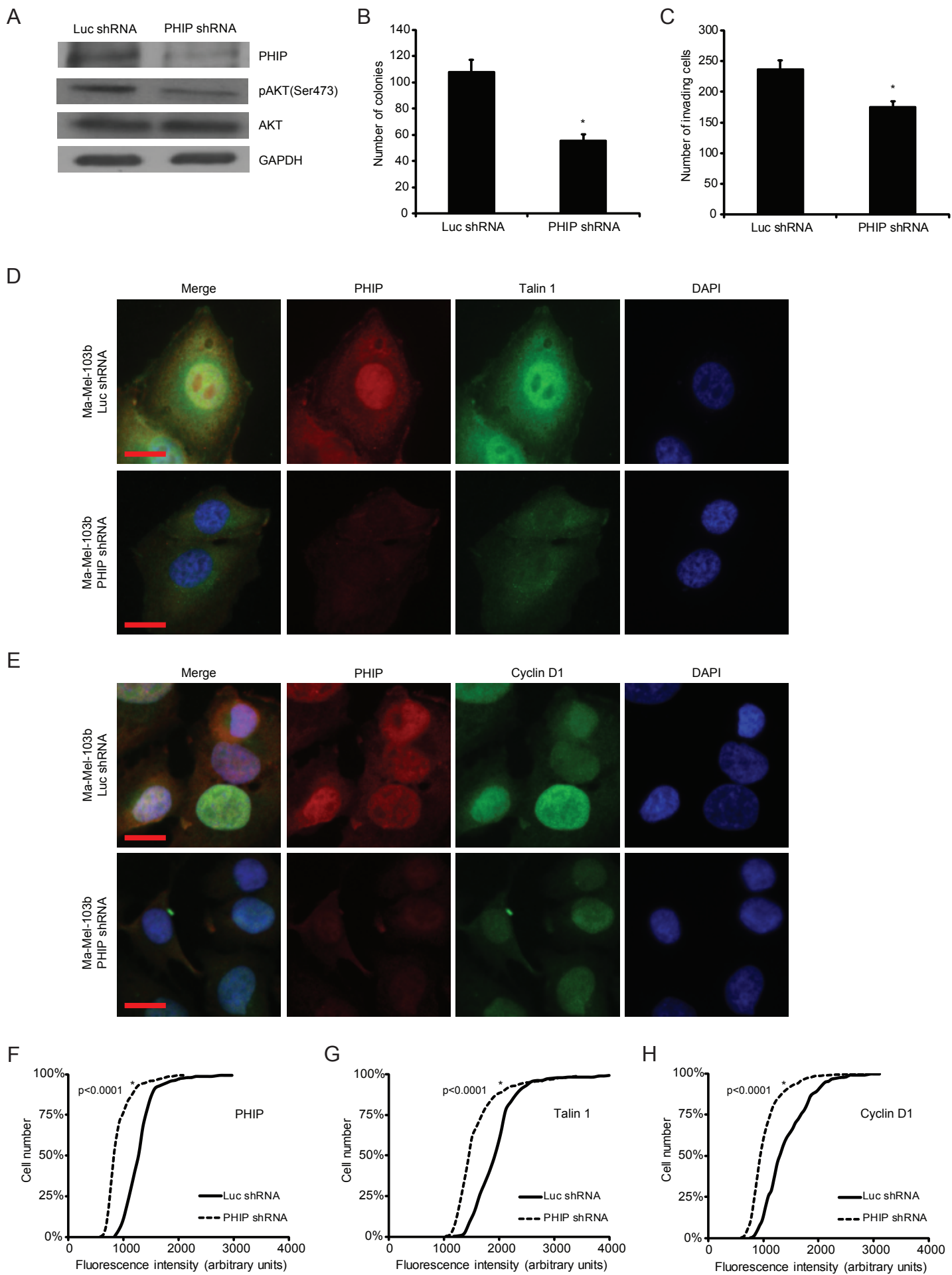


**Fig. S8.** Effects of stable shRNA-mediated suppression of *PHIP* in Ma-Mel-103b cells. (A) Western analysis of expression of PHIP and other proteins in Ma-Mel-103b cells expressing anti-*luc* shRNA or anti-*PHIP* shRNA (127738). (B) Colony formation ability of Ma-Mel-103b cells stably expressing anti-*luc* shRNA or anti-*PHIP* shRNA (127738) ( $P < 0.008$ ). (C) Invasion into Matrigel of Ma-Mel-103b cells expressing anti-*luc* shRNA or anti-*PHIP* shRNA (127738) ( $P < 0.01$ ). (D-E) Qualitative immunofluorescence analysis of (D) PHIP and Talin 1 and (E) PHIP and Cyclin D1 in Ma-Mel-103b cells expressing anti-*luc* shRNA or anti-*PHIP* shRNA (127738) (scale bar, 20 $\mu$ m). (F-H) Quantitative immunofluorescence analysis of (F) PHIP, (G) Talin 1 and (H) Cyclin D1 in Ma-Mel-103b cells expressing anti-*luc* shRNA or anti-*PHIP* shRNA (127738).

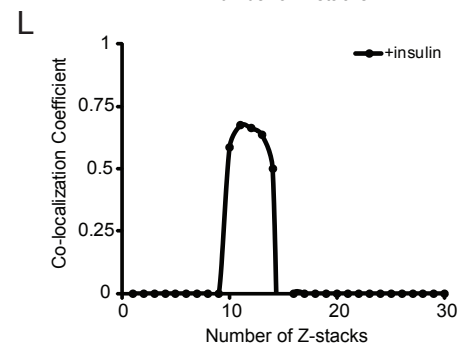
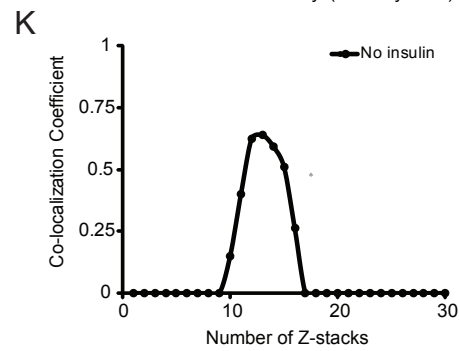
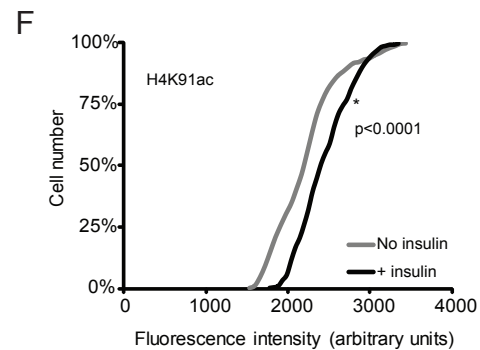
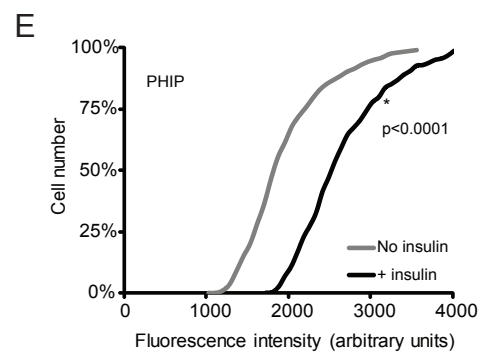
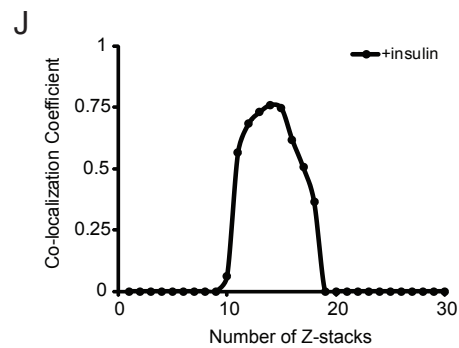
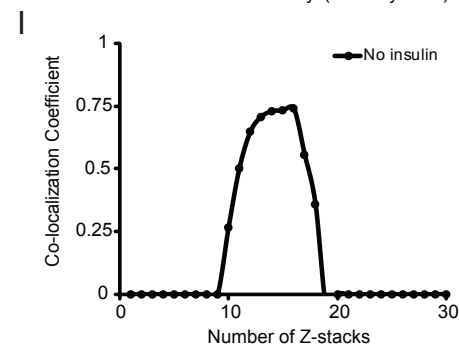
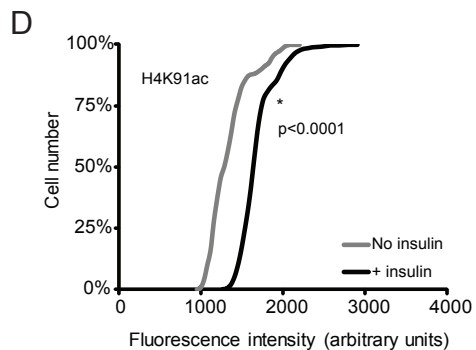
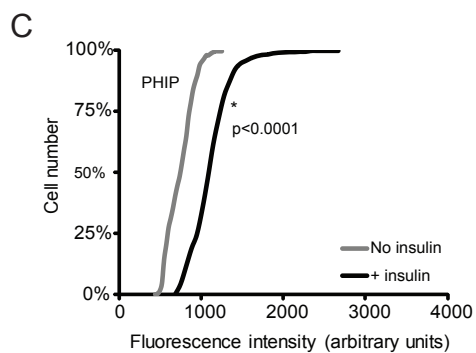
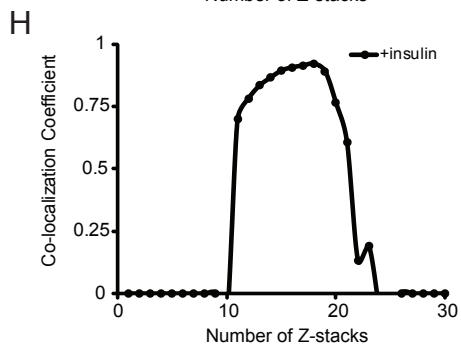
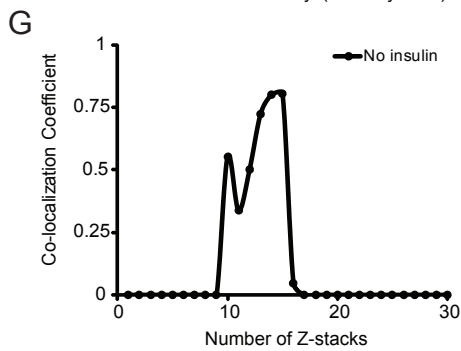
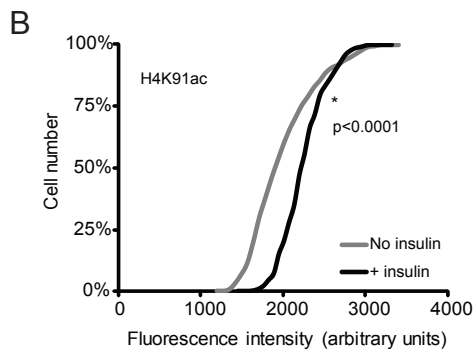
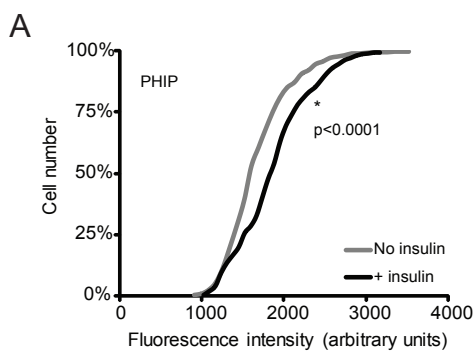


**Fig. S9.** Regulation of expression of PHIP and H4K91ac in MDA-MB-231, H1703, and Ma-Mel-12 cells. (A-F) Quantitative immunofluorescence analysis of PHIP and H4K91ac expression: in MDA-MB-231 cells (A and B), in H1703 cells (C and D) and in Ma-Mel-12 cells (E and F) with or without insulin stimulation, respectively, following overnight starvation. (G-L) Pearson's co-localization coefficient of PHIP and H4K91ac: in MDA-MB-231 cells (G) without or (H) with insulin stimulation; in H1703 cells (I) without or (J) with insulin stimulation; and in Ma-Mel-12 cells (K) without or (L) with insulin stimulation.

**Video S1.** Video rendering of confocal images of MDA-MB-231 cells showing foci of co-localization of PHIP and H4K91ac.

**Video S2.** Video rendering of confocal images of H1703 cells showing foci of co-localization of PHIP and H4K91ac.

**Video S3.** Video rendering of confocal images of Ma-Mel-12 cells showing foci of co-localization of PHIP and H4K91ac.